Neuroscience 558 (2024) 37–49

Contents lists available at ScienceDirect

Neuroscience

journal homepage: www.elsevier.com/locate/nsc

Research Article

Different neural correlates of deception: Crafting high and low creative scams

Xinuo Qiao [a], Wenyu Zhang [a], Ning Hao [a,b,*]

[a] Shanghai Key Laboratory of Mental Health and Psychological Crisis Intervention, School of Psychology and Cognitive Science, East China Normal University, Shanghai 200062, China
[b] Key Laboratory of Philosophy and Social Science of Anhui Province on Adolescent Mental Health and Crisis Intelligence Intervention, Hefei Normal University, Hefei 230601, China

ARTICLE INFO

Keywords:
Creativity
Malevolent creativity
fNIRS
Deception

ABSTRACT

Deception is a complex social behavior that manifests in various forms, including scams. To successfully deceive victims, liars have to continually devise novel scams. This ability to create novel scams represents one kind of malevolent creativity, referred to as lying. This study aimed to explore different neural substrates involved in the generation of high and low creative scams. A total of 40 participants were required to design several creative scams, and their cortical activity was recorded by functional near-infrared spectroscopy. The results revealed that the right frontopolar cortex (FPC) was significantly active in scam generation. This region associated with theory of mind may be a key region for creating novel and complex scams. Moreover, creativity-related regions were positively involved in creative scams, while morality-related areas showed negative involvement. This suggests that individuals might attempt to use malevolent creativity while simultaneously minimizing the influence of moral considerations. The right FPC exhibited increased coupling with the right precentral gyrus during the design of high-harmfulness scams, suggesting a diminished control over immoral thoughts in the generation of harmful scams. Additionally, the perception of the victim's emotions (related to right pre-motor cortex) might diminish the quality of highly original scams. Furthermore, an efficient and cohesive neural coupling state appears to be a key factor in generating high-creativity scams. These findings suggest that the right FPC was crucial in scam creation, highlighting a neural basis for balancing malevolent creativity against moral considerations in high-creativity deception.

Introduction

Deception and malevolent creativity

Deception or fraud is one of the most common unethical behaviors, consistently causing substantial losses to individuals and society (e.g., Bazerman and Gino, 2012; Du and Chen, 2023). The global economy incurs over $5 trillion annually in financial losses due to fraud (Gee and Button, 2019; Hanoch and Wood, 2021), while emotional distress impacts 79 % of scam victims, far exceeding the 24 % who suffer financially (European Commission, 2020). From an individual perspective, self-interested deception can even lead to irreparable damage to relationships (Gaspar et al., 2022; Schweitzer et al., 2006). Overall, deception not only causes significant economic losses but also has profound effects on the psychological health of victims and societal trust.

While existing studies have mostly focused on simplified forms of deceptive behavior within controlled experimental settings—for example, allowing participants to gain more rewards by exaggerating their performance (Cui et al., 2018) or by sending false information to partners (Jenkins et al., 2016)—deception is a complex behavior that interacts with various social factors (Qiao et al., 2023; Walczyk et al., 2008). Accordingly, deception can be seen as a collection of scams, each involving a deliberate blend of deceit and strategy woven into the complex web of social interaction. The working neurological model of deception elucidates the mechanism of scam generation by mapping a cognitive route from the comprehension of relevant information and memory recall to the intricate coordination of planning and decision-

* Corresponding author at: Shanghai Key Laboratory of Mental Health and Psychological Crisis Intervention, School of Psychology and Cognitive Science, East China Normal University, No. 3663, North Zhong Shan Road, Shanghai 200062, China.
E-mail address: nhao@psy.ecnu.edu.cn (N. Hao).

https://doi.org/10.1016/j.neuroscience.2024.08.020
Received 15 April 2024; Accepted 14 August 2024
Available online 17 August 2024

making, thus outlining the neural interplay that governs deceit (Mohamed et al., 2006). Several brain regions proposed in this model, including the prefrontal cortex, right temporo-parietal junction (rTPJ), and angular gyrus (AG, e.g., Lisofsky et al., 2014; Yin et al., 2016), have been found to be associated with deception, particularly linked to the core processes of scam construction: planning and decision-making.

However, a well-planned scam may not be effective in the long term. Cropley et al. (2008) have demonstrated the decay of malevolent behavior (e.g., performing a scam), indicating that its novelty and effectiveness rapidly decrease with the increasing number of implementations. Thus, a scam that has been exposed may be difficult to execute successfully. Deception is regarded as a problem-solving strategy in social situations that requires divergent thinking (Walczyk et al., 2008; Walczyk et al., 2005), and hence, creativity is a key factor in ensuring the success of a scam; scams must continually evolve to maintain their novelty, or they will rapidly lose effectiveness. Progressing further, creativity not only acts as a necessary component but also enhances the "quality" of scams. Previous studies have established that engaging in creativity tasks promote subsequent lying behaviors, the explanation being that both constructing scams and generating novel ideas inherently require breaking established rules (Gino and Ariely, 2012; Walczyk et al., 2008). Moreover, self-interested creative thinking induces individuals to more frequently achieve their goals through deception (Kapoor and Kaufman, 2022). Furthermore, when deception is combined with creativity, random and surprise elements within creativity make scams more difficult for victims to anticipate (Cropley et al., 2008; Gill et al., 2013; Wang, 2019). Moreover creative mindset induces individuals to justify their unethical behaviors, then engage in more deception (Gino and Ariely, 2012; Mai et al., 2015). Integrating the above findings, scammer/liars aim to extract maximum benefits from victims by crafting highly creative scams (DePaulo et al., 2003; Vrij et al., 2010). The successful execution of scams necessitates malevolent creativity, which is the deliberate application of creativity to cause harm (Cropley et al., 2010; Cropley et al., 2008; Harris et al., 2013; Qiao et al., 2022). In particular, they depend on a specific kind of malevolent creativity for scam design: lying (denoted LY in our tests), which involves the creative acts of fabricating lies, concealing truths, and framing others (Hao et al., 2016; Qiao et al., 2023). The LY can be incorporated into the working neurological model of deception, where it plays a role in the planning and decision-making processes of scams (Mohamed et al., 2006).

The neuroscientific findings of creative deception

Currently, most behavioral research on deception considers creativity as an independent factor of influence (e.g., Gino and Ariely, 2012; Kapoor and Khan, 2017), without exploring the creative features inherent to the deception (specifically, LY). At the neural level, the difference in cortical activity was primarily compared to three kinds of malevolent creativity: LY, hurting people and playing trick (Qiao et al., 2023). The study revealed that brain regions associated with theory of mind, particularly the right frontopolar cortex (right FPC), were specifically active in generating novel scams. This is consistent with the predictions of the working neurological model of deception (Mohamed et al., 2006). However, while the previous study preliminarily identified the specific brain regions associated with LY by comparing neural activity among different kinds of MC, it did not consider the varying levels of creativity within the generated scams. Because creativity has been found to be crucial for the successful implementation of a scam (e.g., Walczyk et al., 2008; Walczyk et al., 2005), the current study, within the framework of the working neurological model of deception, further explores the neural substrates involved in planning highly creative scams. Building on the methodology of Qiao et al. (2023), the current study employs various analytical methods (e.g., elastic-net regression and clustering analysis) to further investigate the relationship between neural activity and the generation of highly creative scams. Previous studies have used originality and harmfulness as indicators to measure the creativity level of malevolent ideas (e.g., Perchtold-Stefan et al., 2022, 2023; Qiao et al., 2022). Building on this, the current study aims to compare the differences in neural activity when individuals generate scams with high versus low levels of originality or harmfulness respectively.

Identifying regions of interest in the generation of highly creative scams

Constructing creative scams may involve multiple psychological processes, with key brain regions associated with these processes potentially linked to the neural substrates that underlie scam creation. The working neurological model of deception emphasizes the contribution of prefrontal regions (e.g., DLPFC and FPC) to scam generation through the planning of deceptive behavior and inhibition of honest responses (Mohamed et al., 2006; Yin et al., 2016). Consistent with the model's assumption, previous studies found that lies activated the anterior prefrontal cortex, potentially associated with monitoring victims' behavior (Pinti et al., 2021). Additionally, lying entails reconciling moral and material conflicts, requiring extra cognitive effort, which leads to increased activity within the cognitive control network (including PFC; van 't Veer et al., 2014; Pang et al., 2022; Speer et al., 2020). Theory of mind (ToM) is utilized by liars to shape victims' beliefs, predict their actions, and discern their thoughts (Walczyk and Cockrell, 2022; Walczyk et al., 2014). Corresponding to these findings, ToM-related regions like the TPJ, precuneus, and orbitofrontal cortex are implicated in various deceptions (Carrington and Bailey, 2009; Speer et al., 2022; Thijssen et al., 2017; Zheltyakova et al., 2022).

Creativity, notably malevolent creativity, is a key ability in designing novel scams (Hao et al., 2016). General creativity has been found to positively correlate with or promote deceptive behaviors (e.g., Gino and Ariely, 2012; Kapoor and Khan, 2017). Thus, the generation of creative scams may elicit neural responses in regions associated with creativity. The executive control network (e.g., the frontal regions), which is vital for working memory and task-switching, supports the generation of creative ideas (Beaty et al., 2016; Zhu et al., 2017). Concurrently, creativity relies on the default network for the retrieval of memories (e.g., rTPJ) and the integration of information (e.g., angular gyrus; Fink et al., 2010; Zhu et al., 2017). Moreover, the executive control network collaborates with the default network to regulate prominent responses triggered by memory retrieval (Beaty et al., 2017). Generating novel scams, as a manifestation of malevolent creativity, may involve brain regions associated with malevolent creation. Malevolent idea generation is associated with reduced involvement of middle occipital gyrus (MOG) indicating decline in moral criteria (Qiao et al., 2022) and postcentral gyrus, indicating weakened emotional perception (Gao et al., 2022). Individuals exhibiting high levels of malevolent creativity displayed increased alpha power in the prefrontal region during the early stage of generating malevolent ideas (signifying the transition from prosocial to antisocial thinking) and increased alpha power in the temporal region (denoting the restraint of conventional, dominant concepts; Perchtold-Stefan et al., 2023) during the middle stage. Integrating the above studies, the key brain regions for generating novel scams may be located in the bilateral prefrontal cortex (e.g., DLPFC and anterior frontal cortex) and the right temporal lobe (i.e., right TPJ and precuneus).

The current study

The current study aims to explore the neural correlates of generating highly creative scams by comparing cortical activity associated with generating highly, versus less creative, scams. Participants were required to complete lying tasks (LYT), during which they were instructed to generate novel scams for various scenarios. Hunter et al. (2022) have indicated that not all deceptive behaviors qualify as malevolent creativity (i.e., they do not all involve the subjective intention to harm others). To highlight the antisocial features of lying (i.e.,

causing deliberate harm), the LYT used in the current study explicitly indicates the intention of harming others to gain personal benefit. Functional near-infrared spectroscopy (fNIRS) was utilized to capture neural activity throughout the LYT. This method offers multiple benefits, including its: (1) resilience to bodily movements (Schecklmann et al., 2010), (2) enhanced ecological validity, and (3) cost-effectiveness. Initially, channels that were significantly activated relative to baseline during LYT were identified. Then, neural activation and coupling were compared between the generation of high and low originality/harmfulness lying ideas. Subsequently, Pearson correlation analysis and elastic-net regression were performed to examine the difference in the behavior-neural relationship between the generation of high and low originality/harmfulness lying ideas. Further, the clustering analysis (including sliding window approach and k-means clustering) was adopted to extract the neural coupling states of high- and low-creativity lying. Several metrics such as ratio, number of transition and dwell time were calculated to characterize the identified states, while graph-based metrics including global and local efficiency were used to measure the network efficiency of each state. Considering the limited neuroscience research on novel deception, we presently propose a more generalized hypothesis. We hypothesize that (1) differences in neural activity (i.e., neural activation and neural coupling) when generating high- or low-creativity scams would be observed in the bilateral prefrontal cortex and temporal cortex, particularly in the right FPC and right MOG; (2) high-creativity lying would be more closely associated with creativity-related and deception-related regions than low-creativity lying; (3) the generation of high-creativity scams would be related to neural coupling states with high efficiency. In addition, several factors were demonstrated that can affect generation of lying creation, including general creativity potential (e.g., Gino and Ariely, 2012; Kapoor and Khan, 2017), malevolent creativity potential (e.g., DePaulo et al., 2003; Qiao et al., 2023; Vrij et al., 2010) and moral personality (e.g., Kapoor and Kaufman, 2022; Qiao et al., 2023). Therefore, these factors were measured by scales to examine their effects on neural correlates underlying scam generation.

Method

Participants

The present study used behavioral and fNIRS data that previously published in Qiao et al. (2023). The data of 40 participants (mean age = 21.30 ± 2.23 years; 32 females; college students) were analyzed. A priori power analysis indicated that a sample size of 36 would be sufficient to obtain reliable results ($1 - \beta = 0.90$, $\alpha = 0.05$, effect size $f = 0.25$; Chow et al., 2017). This sample size is in line with those employed in previous neuroscientific creativity studies (e.g., Jiang et al., 2023; Ren et al., 2023; Takeuchi et al., 2019; Tempest and Radel, 2019; Xie et al., 2021). All the participants were right-handed and had normal or corrected-to-normal visual acuity. None of the patients had any history of mental or neurological illness. Written informed consent was obtained from all participants before the experiment. The study procedure was approved by the University Committee on Human Research Protection of the East China Normal University (Code: HR 039-2017).

Experimental procedure

Upon arrival, each participant would be provided with informed consent. After participants signed the hard copy of consent and agreed to proceed the experiment, the experimenter would introduce the whole procedure to them and prepared the fNIRS device.

The formal procedure started with a 30-second baseline scanning session, during which participants were instructed to close their eyes, remain still, and relax. Then, participants completed 10 randomized lying tasks (see details in *The development and assessment of lying tasks*). Each task trial consisted of an 8 s fixation session, a 10-second task-reading session, a 20-second thinking session, and a 12-second reporting session. While participants could mentally conceive multiple responses, they were only required to verbally report the most creative during the reporting session. Two jitters (blank screen, 2–6 s) were set between the task-reading, thinking and reporting three sessions (Fig. 1).

Immediately after completing the lying tasks, the participants rated their anxiety, pleasure, and tasks' benevolence and malevolence on a 7-point Likert scale ranging from 1 (not at all) to 7 (strongly). Finally, the participants were asked to complete a series of scales immediately after they finished the whole experiment (see details in the "*Traits*" section).

The development and assessment of lying tasks

The lying tasks in this study, derived from a Realistic Presented Problem (RPP) format, involved generating creative solutions for open-ended realistic problems (Agnoli et al., 2016; Runco et al., 2016; Xue et al., 2018). Ten distinctive lying tasks were utilized. Each task was constrained to 38–42 Chinese characters to maintain consistency. Participants were instructed to address the tasks through innovative lying, concealing, and framing strategies (e.g., Ming wishes to acquire a luxury watch but cannot afford it. Please generate a novel strategy for Ming to cunningly solicit donations from others). The efficacy of these lying tasks has been validated in earlier research (Cheng et al., 2021b; Qiao et al., 2023).

Performances of lying tasks were assessed by evaluating the originality and harmfulness of the ideas (Runco and Okuda, 1991; Gao et al., 2022; Perchtold-Stefan et al., 2020, 2022; Qiao et al., 2022; Qiao et al., 2023). A subjective method, commonly applied in creativity research, was employed to evaluate the originality and harmfulness of these ideas (Beaty et al., 2018; Lu et al., 2019; Xue et al., 2018). Five independent trained raters (with at least three years of experience in creativity research) scored originality and harmfulness of each idea on a 5-point Likert scale (originality: 1 = not original at all, 5 = highly original; harmfulness: 1 = not harmful at all, 5 = highly harmful). The inter-rater agreement was satisfactory, with internal consistency coefficients of 0.70 for originality and 0.74 for harmfulness. The originality and harmfulness scores for each idea were calculated by averaging the scores from five raters.

The high and low creative lying ideas were determined by the score of originality or harmfulness within each lying task (Fig. 2A). Given that 40 participants were recruited in this study, a total of 40 data (i.e., 40 values of originality and harmfulness respectively) were obtained for each lying task. For originality, ideas surpassing the mean originality score for a given task were classified as high-originality, while those below the mean were classified as low-originality.

In respect of originality, if the originality of an idea is higher than the mean score of originality within a single lying task, it will be classified as a high-originality idea; if the originality of an idea is lower than the mean value of originality within single lying task, it will be classified as low-originality idea. For example, one LYT scenario used in the study: Ming works part-time at an educational institution and wants to improve his sales performance. Devise a novel way to deceive his classmates into believing that they will fail their exams if they do not attend extra classes at the institution. For this task, a high-originality idea: secretly spread rumors in the class that the final exam is very difficult, and that the teachers have made an agreement with the institution that students will fail if they do not attend extra classes; a low-originality idea: individually tell every classmate that they must attend the extra classes, or they will fail. Similarly, ideas were classified as high-harmfulness or low-harmfulness based on the same procedure. Example LYT: Ming wants to bribe the school authorities but does not have enough money. Devise a novel way for Ming to deceive his roommate into willingly giving him the money for this purpose. High-harmfulness idea: exploit a negative secret about the roommate and tell him that the school authorities are already aware of it, but if they bribe the authorities, they will overlook the issue; low-harmfulness idea: tell the roommate that Ming greatly

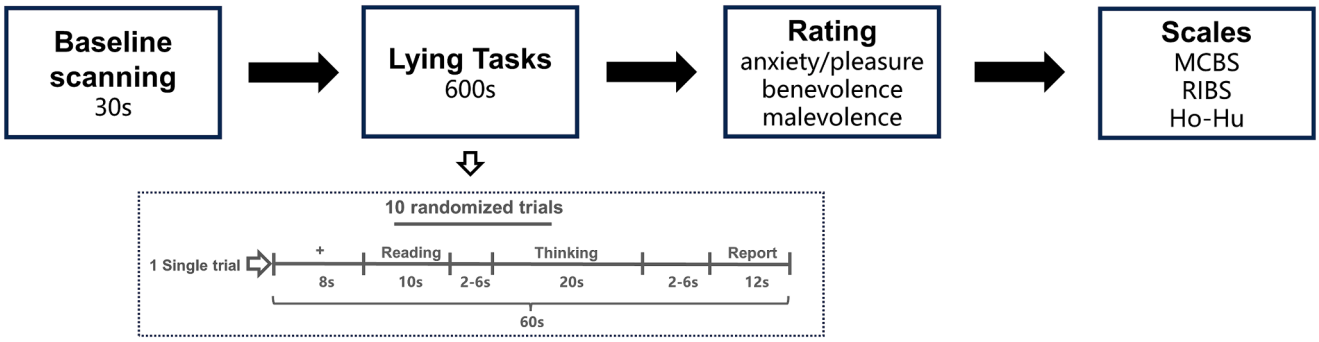

Fig. 1. The flow chart of experimental procedure. MCBS = Malevolent Creativity Behavior Scale; RIBS = Runco Ideational Behavior Scale; Ho-Hu = Honesty-Humility Inventory.

admires the school authorities and wants to give him a gift, but is currently short of money, and hopes the roommate can help.

The neural activity associated with generating high and low creativity lying ideas will be analyzed separately.

For each participant, the overall originality and harmfulness scores were determined by averaging the scores of all ideas generated by them. The final scores for high originality/harmfulness were computed by averaging the scores of all ideas classified as such, while final scores for low originality/harmfulness were similarly calculated based on ideas classified under these criteria.

Traits

The lying subscale of Malevolent Creativity Behavior Scale (MCBS) e.g. *It is easy for me to tell a lie and I can justify it perfectly* (Hao et al., 2016) was used to evaluate the participants' potential of generating creative lies. The lying subscale contains 4 items rated on a 5-point Likert scale ranging from 1 (never) to 5 (always). The internal consistency reliability was satisfactory (Cronbach's $\alpha = 0.74$). The Runco Ideational Behavior Scale (RIBS) e.g. *I have a lot of ideas about a new invention* (Runco et al., 2016) was used to evaluate the participants' general creativity potential. The RIBS contains 19 items rated on a 5-point Likert scale ranging from 0 (never) to 4 (approximately every day). The internal consistency reliability was satisfactory (Cronbach's $\alpha = 0.88$). The Honesty-Humility Inventory (Ho-Hu) e.g. *If money is tight, I can't resist the temptation to buy stolen goods* (Lee and Ashton, 2004) was used to evaluate the participants' moral personalities. The Ho-Hu contains 20 items rated on a 5-point Likert scale ranging from 1 (strongly disagree) to 5 (strongly agree). The internal consistency reliability was satisfactory (Cronbach's $\alpha = 0.78$).

fNIRS data acquisition

In this study, the bilateral PFC and right temporal cortex (include right TPJ) were selected as regions of interest (ROI). A 3 × 5 probe set (22 measurement channels; eight emitters and seven detectors, 3 cm optode separation; Fig. 2B) was positioned on the bilateral PFC, while a 4 × 4 probe set (24 measurement channels; eight emitters and eight detectors, 3 cm optode separation; Fig. 2C) was positioned on the right temporal cortex. The layout of these two probe sets was based on the 10–20 system: the lowest row of the 3 × 5 probe set was aligned with the Fp1–Fp2 line, with optode 'A' positioned at the frontal pole midline point (Fpz; Sai et al., 2014), and the middle probe column of the 3 × 5 set aligned along the sagittal reference curve (Fig. 2B). The 4 × 4 set was aligned with the sagittal reference curve, positioning optode 'B' on P6 (Fig. 2C). The virtual registration method established the correspondence between measurement channels and cortical brain regions in the ROI (Singh et al., 2005; Tsuzuki et al., 2007).

During the experiment, an fNIRS device (ETG-7100, Hitachi Medical Corporation, Japan) measured the concentrations of oxyhemoglobin (HbO) and deoxyhemoglobin (HbR) in the ROI. It specifically assessed the absorption of near-infrared light at wavelengths of 695 and 830 nm, with a sampling rate of 10 Hz.

fNIRS data pre-processing

The pre-processing procedure included following steps contained in Cui et al., 2012 and Pan et al., 2018 (Fig. 2D): (1) Application of the principal component spatial filter algorithm to remove global components from the raw data; (2) Use of correlation-based signal improvement to eliminate motion artifacts. After correction, oxy-hemoglobin (HbO) and deoxy-hemoglobin (HbR) were found to be negatively correlated (i.e., corrected HbR values equaled the products of corrected HbO and a negative coefficient; Cui et al., 2010). Therefore, data analysis primarily focused on HbO rather than HbR; (3) Identification and selection of channels with poor signals. Poor channels were determined through visual inspection using NIRS time-course plots, identifying channels with significantly higher variance compared to others in the same participant (e.g., normal channel variances ranged from 0.5 to 0.8, whereas poor channels ranged from 10 to 30). Participants with more than 11 poor channels, exceeding 25 % of total channels, were excluded from further analysis.

Estimation of neural activation

Generally, the neural activation within each channel of the ROI during the thinking phase was analyzed using the NIRS Statistical Parametric Mapping (NIRS_SPM) software package (Jang et al., 2009; Ye et al., 2009). As mandated by the NIRS_SPM, the hemodynamic response function (hrf) low pass filtering and wavelet minimum description length detrending algorithms were employed. The general linear model was used to estimate neural activation.

The neural activation during the thinking stage of all lying tasks was estimated through the following steps (Fig. 2D); (1) A reference wave was established for each channel to reflect the theoretical changes in HbO signals triggered by the experimental stimulus, namely generating creative lying ideas; (2) A regression analysis was conducted for each channel, incorporating both theoretical and actual HbO signal variations during the baseline and thinking phases of lying tasks; (3) Beta (β) values, serving as regression coefficients, were calculated to represent changes in neural activation across all channels during both baseline and lying tasks; (4) the beta increment was further calculated by subtracting the baseline beta value from the thinking-session beta value for lying tasks; (5) To assess the increase in neural activation specifically during the lying tasks, the beta increment was calculated by deducting the baseline beta value from the thinking-phase beta value; (6) Beta increments were then standardized using Z-score transformation for each channel across all participants.

Next, a similar procedure was applied to estimate the neural activation associated with the generation of both high-originality and low-

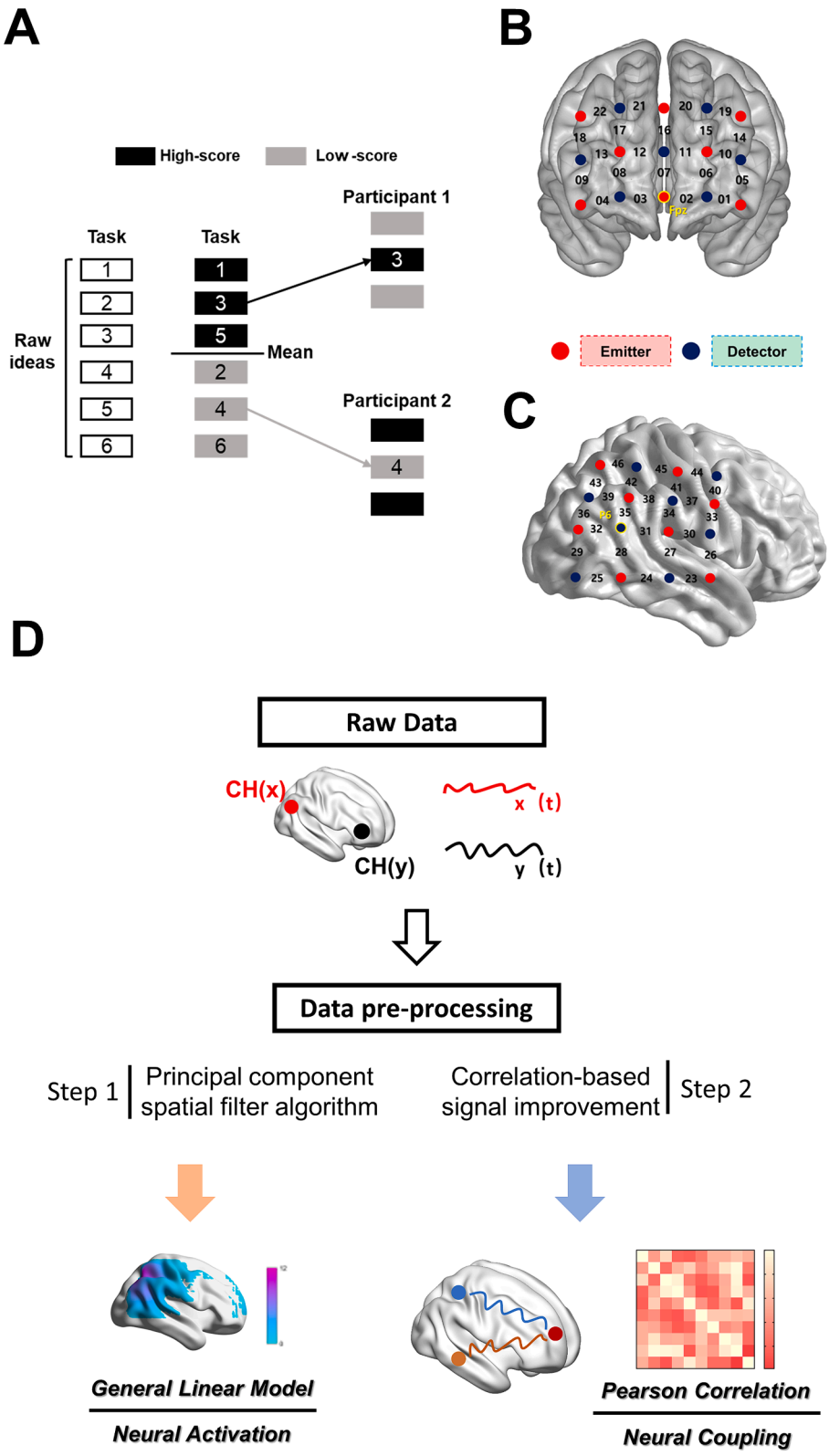

Fig. 2. (A) The procedure of classification of high- and low-creativity ideas; (B) Optode probe set on the prefrontal cortex; (C) Optode probe set on the right temporal regions; (D) the data pre-processing and analysis procedure.

originality ideas: (1) Two reference waves were established for each channel, reflecting the theoretical HbO signal changes for both high- and low-originality ideas; (2) A regression analysis was conducted for each channel, incorporating both theoretical and actual HbO signal changes (e.g., baseline, thinking stage of high- and low-originality ideas); (3) Beta values were calculated to represent the changes in neural activation across all channels during baseline, and the generation of high-, and low-originality ideas, respectively; (4) The beta increments were calculated to assess the increase in neural activation specifically during the generation of high- and low-originality ideas; (5) the beta increments of

high- and low-originality ideas were Z-scores, transformed channel by channel, across the participants. Finally, the neural activation pertaining to high- and low-harmfulness ideas was assessed using the same procedure as for originality.

Estimation of neural coupling

Neural coupling (NC) indicates the functional connectivity between different cerebral regions during the thinking stage of lying tasks. Neural coupling strength was quantified using correlation coefficients (Fig. 2D). Pearson correlations were employed to evaluate the NC between HbO signals from each channel pair (e.g., Gao et al., 2022). Initially, 2,116 channel (CH) combinations (46 × 46 CHs) were identified. After excluding 1,081 redundant CH combinations (equal CH combinations [e.g., CH1-CH2 and CH2-CH1] or CH combinations of a single CH [e.g., CH1-CH1]), 1,035 valid CH combinations remained. Next, NC values (i.e., correlation coefficients) were converted using Fisher's z-transformation. Similar to beta increments, NC values were calculated for all types of idea, including high-originality/high-harmfulness and low-originality/low-harmfulness lying ideas.

Difference comparison in neural activity during lying tasks

A total of 46 (channel) one-sample t-tests using 0 as the test value (i.e., baseline) were performed on the beta increments of lying tasks (Fig. 2D). These analyses identified channels that were significantly activated or deactivated during the lying tasks. All *p*-values were corrected using the false discovery rate correction method (FDR; corrected alpha level = 0.05).

Next, the differences in neural activity (i.e., beta increments and NC values) during the generation of high- and low-creativity ideas were examined: (1) A series of paired-sample t-tests (46 for beta increments and 1035 for NC values) compared the difference in neural activity between the generation of high- and low-originality ideas; (2) Another set of paired-sample t-tests (46 for beta increments and 1035 for NC values) were conducted to compare the difference in neural activity between high- and low-harmfulness ideas.

The next stage was the investigation of differences in the relationship between neural activity and lying task performance when generating ideas of high and low creativity. Pearson correlation analyses were used to calculate the correlation coefficients between the originality scores of high- or low-originality ideas and their corresponding beta increments. Furthermore, a selection criterion for the *p* value was set at 0.05 ($p < 0.05$, uncorrected); a channel that passes the selection criteria in at least one of the two correlation relationships between the originality scores of high- or low-originality ideas and the corresponding beta increments will be entered into subsequent analyses. Fisher's Z tests were performed to examine the difference in strength of task performance-beta increment relation between high- and low-originality ideas. All *p*-values of Fisher's Z tests were corrected using the FDR method (corrected alpha level, 0.05). The same procedure will be applied to high- and low-harmfulness. A similar analyses procedure was performed on NC values for each CH combination (except the selection criterion was set to 0.005, uncorrected). Moreover, the differences in the relationship between traits and neural activity when generating ideas of high- and low-creativity (i.e., originality and harmfulness) was investigated with the abovementioned method.

Elastic-net regression

Elastic net regression was used to examine which brain regions or inter-regional neural activities could significantly predict task performance. It was separately conducted for high-creativity (i.e., high-originality/harmfulness) and low-creativity ideas (i.e., low-originality/harmfulness). This type of regression was suitable when predictors outnumber dependent variables (Xie et al., 2022). Next, the analysis procedure was illustrated using high-originality ideas and beta increments as examples. Before the formal procedure of elastic-net regression, several Pearson correlation analyses were performed on originality scores of high-originality ideas and beta increments of each channel. Only the channel that significantly correlated with originality ($p < 0.05$, uncorrected) would be introduced into subsequent elastic-net regression as predictors (Xie et al., 2022). Elastic-net regression contains two parameters: α and λ. The parameter α ranges from 0 to 1, which indicates the proportion of ridge and LASSO (Least absolute shrinkage and selection operator regression) penalization (Zou and Hastie, 2005). When α is 0, elastic-net regression converts into ridge regression; when α is 1, elastic-net regression converts into LASSO regression. The parameter λ is a positive value that indicates the severity of penalty. Elastic-net regression converts into ordinary least squares regression when λ is 0, whereas the weights of all predictors become 0 when λ is maximized. In the current study, elastic-net regression was performed on every behavioral performance respectively (with beta increments as predictors). The values of α were set between 0.001 and 1 (in steps of 0.001, a total of 1000 α values; for example, α could be 0.002 and 0.003). For each α value, elastic-net regression models with different λ values were established (the λ value was gradually increased from 0 until the weights of all predictors become 0). Next, the leave one out cross-validation (LOOCV) was used to select an optimal elastic-net model with minimal mean square error for each behavioral performance (Xie et al., 2022). The predictors that remained in the final optimal elastic-net regression model were considered as dependent variables that significantly predict. The same procedure was applied to high- and low-harmfulness. A similar analyses procedure was also performed on NC values and lying task performance (except the selection criterion was set to 0.005, uncorrected).

Clustering analysis

Clustering analysis was used to identify the NC states during the thinking stage of lying tasks (e.g., Allen et al., 2014; Wang et al., 2022; Fig. 3). Primarily, a sliding window approach generated a series of windowed NC matrices throughout the summary thinking stage, which included baseline, high- and low-creativity ideas. The window size was set to 2 s, and moved in an increment of 0.5 s throughout the summary thinking stage. The 700 s summary thinking stage was then split into 1035 (valid CH combinations) × 136 (quantity of windows) windowed NC matrices for each participant. The same procedure of clustering analysis was performed on originality and harmfulness respectively.

Next, the different NC states were extracted through the following steps: (1) Chained NC matrices across participants were averaged; (2) The k-means clustering method based on MATLAB was used to assess the similarity between windowed NC matrices to identify representative NC states. The similarity was quantified by Manhattan distance (Aggarwal et al., 2001). Various validity indices (i.e., the ratio of within-cluster distance to between-cluster distance) were calculated for an array of state numbers. These validity indices were plotted as a function of state number, then the number of NC states (i.e., clusters) were decided using the elbow criterion (i.e., the state number is chosen at the elbow of the curve to best balance the cost of clustering, e.g., Fang et al., 2020; Li et al., 2021); (3) An iteration process, conducted one thousand times, calculated the cluster centroids for representative NC states across all participants; (4) Cluster centroids derived from step (3) served as the initial centroids for the clustering analysis of individual participants, yielding the final NC states for each.

Following the determination of NC states for each participant, various metrics were employed to characterize these states (Li et al., 2021; Wang et al., 2022): (1) The ratio of each state, indicating the percentage of total windows accounted for by each state; (2) The number of transitions between states, indicating the frequency of switches between different states; (3) the dwell time of each state, representing the mean duration spent in each state (measured from every

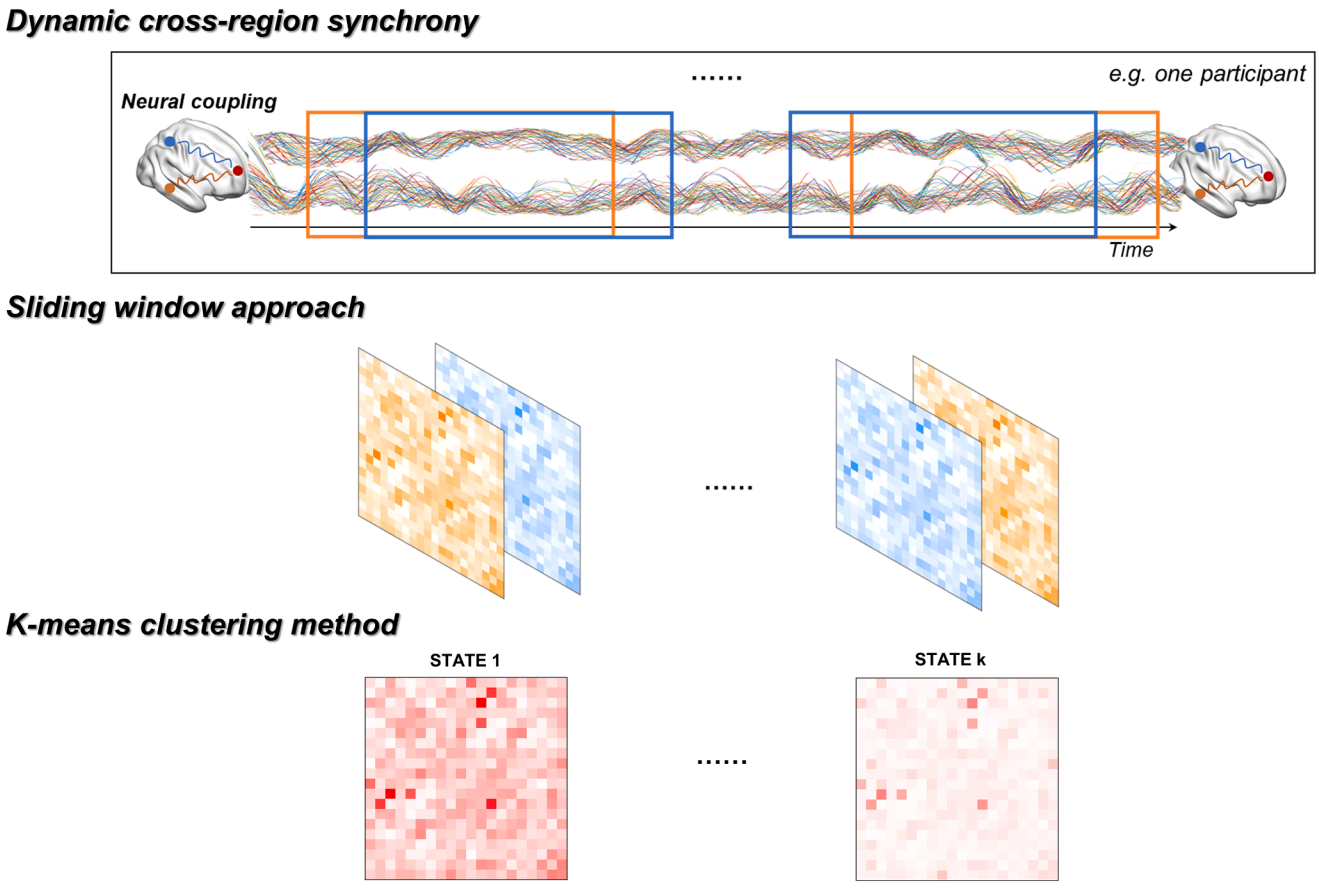

Fig. 3. The clustering analysis procedure.

start point). The graph-based metrics were computed by GRETNA in MATLAB (Achard and Bullmore, 2007; He et al., 2009; Wang et al., 2015): global (globE) and local efficiency (locE), measuring the efficiency of parallel information transfer globally and locally. Several paired t-tests were performed to examine the difference in the above-mentioned metrics between generating high-creativity (i.e., high-originality and high-harmfulness) and low-creativity (i.e., low-originality and low-harmfulness) lying ideas. All *p*-values were corrected using the FDR method (corrected alpha level, 0.05).

Results

Effectiveness of idea classification

The generated ideas were classified into high-originality/high-harmfulness and low-originality/low-harmfulness ideas. Two paired t-tests using group (high-originality vs. low-originality/ high-harmfulness vs. low harmfulness) as the independent variable were performed on scores of lying task performance. Results revealed that the score of originality in high-originality ideas ($M = 2.66$, $SD = 0.29$) was significantly higher than low-originality ideas ($M = 1.41$, $SD = 0.70$; $t\ (39) = 11.94$, $p < 0.001$); the score of harmfulness in high-harmfulness ideas ($M = 2.69$, $SD = 0.28$) was significantly higher than low- harmfulness ideas ($M = 1.45$, $SD = 0.76$; $t\ (39) = 11.86$, $p < 0.001$). These results indicated that the idea classification in the current study was effective.

Baseline analysis

One-sample t-tests using 0 as the test value (baseline) were performed on the beta increments among all the CHs (see details in Table 1). After FDR correction ($p < 0.05$, a total of 46 channels), the results revealed that the bilateral FPC (CH2, CH3, and CH4), right middle occipital gyrus (rMOG; CH36), right AG (CH39), and right precuneus (CH43 and CH46) were more activated than baseline; the right DLPFC (rDLPFC; CH16), right middle temporal gyrus (CH23), right superior temporal gyrus (CH27), right postcentral gyrus (rPOG; CH30), and right supramarginal gyrus (rSMG; CH34) were less activated than baseline (Table 1).

Table 1
Results of One-Sample T-test on beta Increment.

Channel	*t*	p_{fdr}	Region
2	3.91	0.004	Left FPC
3	5.34	<0.001	Right FPC
4	5.18	<0.001	Right FPC
16	−2.91	0.025	Right DLPFC
23	−3.87	0.004	Right MTG
27	−3.25	0.012	Right STG
30	−3.45	0.009	Right POG
34	−3.60	0.007	Right SMG
36	2.81	0.030	Right MOG
39	3.16	0.014	Right AG
43	4.67	0.001	Right precunes
46	3.35	0.010	Right precunes

Note. Only channels that significant different from baseline were listed below. The *p* values were FDR corrected. FPC = frontopolar cortex; DLPFC = dorsolateral prefrontal cortex; MTG = middle temporal gyrus; STG = superior temporal gyrus; POG = postcentral gyrus; SMG = supramarginal gyrus; MOG = middle occipital gyrus; AG = angular gyrus.

Differences in neural activity

A total of 46 paired-sample t-tests were performed to examine the

differences in beta increments between generation of high- and low-originality lying ideas. After FDR correction, the differences between high- and low-originality lying ideas were not significant for any channel. Another set of paired-sample t-tests were performed on high- and low-harmfulness lying ideas, for which the differences in beta increments between generation of high- and low-harmfulness lying ideas were not significant for any channel.

A total of 1035 paired-sample t-tests were performed to examine the differences in NC values between generation of high- and low-originality lying ideas. After FDR correction, the differences between high- and low-originality lying ideas were insignificant for all CH combinations. Another set of paired-sample t-tests were performed on high- and low-harmfulness lying ideas, here the NC values of CH7-CH44 (rFPC-right precentral gyrus) were higher during generation of high-harmfulness lying ideas ($M = 0.26$, $SD = 0.29$) than during low-harmfulness lying ideas ($M = -0.03$, $SD = 0.35$; t (39) = 4.73, $p_{fdr} = 0.031$; Fig. 4A).

Differences in correlation coefficients

The Fisher's Z tests were used to examine the difference in task performance-neural activity relationship between high- and low-creativity lying ideas (see detailed procedure in *Difference comparison in neural activity during lying tasks*). The significant differences were only observed in originality-neural activity relation and not harmfulness-neural activity relation.

For originality-neural activation, results revealed that the correlation coefficient between originality and beta increment in CH40 (i.e., right pre-motor cortex) was lower during high-originality ($r = -0.35$, $p = 0.026$) than during low-originality lying ideas ($r = 0.16$, $p = 0.316$; $p_{FiserZ\text{-}fdr} = 0.037$).

For originality-neural coupling, results revealed that the correlation coefficient between originality and NC value in CH9-CH11 (i.e., rDLPFC-left DLPFC) was higher during low-originality ($r = 0.44$, $p = 0.004$) than high-originality lying ideas ($r = -0.16$, $p = 0.336$; $p_{FiserZ\text{-}fdr} = 0.035$); the correlation coefficient between originality and NC value in CH17-CH24 (i.e., rDLPFC-right fusiform gyrus) was lower during low-originality ($r = -0.48$, $p = 0.002$) than high-originality lying ideas ($r = 0.13$, $p = 0.432$; $p_{FiserZ\text{-}fdr} = 0.039$).

Next, the differences between high- and low-creativity lying ideas in trait- neural activity relationship were also examined by Fisher's Z test. The correlation coefficient between RIBS and NC value in CH6-CH44 (i.e., left FPC-right precentral gyrus) was higher during high-originality ($r = 0.46$, $p = 0.003$) than low-originality lying ideas ($r = -0.07$, $p = 0.657$; $p_{FiserZ\text{-}fdr} = 0.050$); the correlation coefficient between Ho-Hu and NC value in CH14-CH30 (i.e., left inferior frontal gyrus-right postcentral gyrus) was higher during low-harmfulness ($r = 0.47$, $p = 0.002$) than high-harmfulness lying ideas ($r = -0.15$, $p = 0.467$; $p_{FiserZ\text{-}fdr} = 0.038$); the correlation coefficient between Ho-Hu and NC value in CH11-CH43 (i.e., left FPC-right precuneus) was lower during high-originality ($r = -0.59$, $p < 0.001$) than low-originality lying ideas ($r = 0.05$, $p = 0.755$; $p_{FiserZ\text{-}fdr} = 0.016$).

Results of elastic-net regression

Elastic-net regression was used to quantify the relationship between the neural activity (beta increments and NC values) and task performances (i.e., the originality and harmfulness of lying tasks).

For beta increments, the originality of high-originality scams ($\alpha = 0.001$, $\lambda = 0.46$, MSE = 0.07) was positively predicted by the beta increments of CH5 (left DLPFC; $b = 2.24$), while negatively predicted by the beta increment of CH36 (rMOG; $b = -1.19$); the originality of low-originality scams ($\alpha = 0.001$, $\lambda = 0.19$, MSE = 0.65) was negatively predicted by beta increment of CH36 (right MOG; $b = -3.82$). No meaningful results were found in harmfulness.

For NC values, the originality of high-originality scams ($\alpha = 0.001$, $\lambda = 0.47$, MSE = 0.04) was positively predicted by the NC values of CH15-CH30 (left DLPFC-right precentral gyrus; $b = 0.14$); the originality of low-originality scams ($\alpha = 0.001$, $\lambda = 0.65$, MSE = 0.10) was negatively predicted by the NC values of CH17-CH24 (right DLPFC-right fusiform gyrus; $b = -0.24$); the harmfulness of high-harmfulness scams ($\alpha = 0.001$, $\lambda = 0.38$, MSE = 0.03) was negatively predicted by the NC values of CH25-CH30 (right MOG-right precentral gyrus; $b = -0.16$); the harmfulness of low-harmfulness scams ($\alpha = 0.001$, $\lambda = 0.18$, MSE = 0.42) was negatively predicted by the NC values of CH21-CH35 (right DLPFC-right AG; $b = -2.74$).

Results of clustering analysis

The neural coupling during baseline, high-, and low-originality idea generation, were clustered together to identify representative NC states. After the comparison of differences in graph-based metrics between NC states, the differences across baseline, high-originality, and low-originality ideas were examined.

For originality, two distinctive NC states (i.e., State 1 and State 2) were extracted (Fig. 4B). Results of paired t-test revealed that the global efficiency was higher in State 2 ($M = 1.77$, $SD = 0.01$) than State 1 ($M = 1.64$, $SD = 0.01$; $t(39) = 9.49$, $p < 0.001$); the local efficiency was higher in State 2 ($M = 0.40$, $SD = 0.01$) than State 1 ($M = 0.34$, $SD = 0.03$; $t(39) = 16.94$, $p < 0.001$). Further, the one-way ANOVAs were used to examine the differences in various metrics. Results revealed that the ratio of State 1 during high-originality idea generation ($M = 0.89$, $SD = 0.05$; $F = 6.59$, $p = 0.002$, $\eta_p^2 = 0.14$) was significantly lower than during baseline ($M = 0.91$, $SD = 0.04$; Bonferroni corrected: $p = 0.011$); the ratio of State 2 during high-originality idea generation ($M = 0.11$, $SD = 0.05$; $F = 6.59$, $p = 0.002$, $\eta_p^2 = 0.14$) was significantly higher than during baseline ($M = 0.09$, $SD = 0.04$; Bonferroni corrected: $p = 0.011$).

For harmfulness, two distinctive NC states (i.e., State 1 and State 2) were extracted (Fig. 4C). The paired t-tests give a global efficiency higher in State 2 ($M = 1.77$, $SD = 0.01$) than State 1 ($M = 1.64$, $SD = 0.01$; $t(39) = 8.66$, $p < 0.001$); the local efficiency was higher in State 2 ($M = 0.40$, $SD = 0.01$) than State 1 ($M = 0.34$, $SD = 0.03$; $t(39) = 17.34$, $p < 0.001$). Further, the one-way ANOVAs were used to examine the differences in various metrics. The dwell ratio of State 1 during high-harmfulness idea generation ($M = 0.87$, $SD = 0.07$; $F = 8.35$, $p = 0.001$, $\eta_p^2 = 0.18$) was significantly lower than during low-harmfulness idea generation ($M = 0.90$, $SD = 0.04$; Bonferroni corrected: $p = 0.040$) and baseline ($M = 0.91$, $SD = 0.04$; Bonferroni corrected: $p = 0.006$); the ratio of State 2 during high-harmfulness idea generation ($M = 0.13$, $SD = 0.07$; $F = 8.35$, $p = 0.001$, $\eta_p^2 = 0.18$) was significantly higher than during low-harmfulness idea generation ($M = 0.10$, $SD = 0.04$; Bonferroni corrected: $p = 0.040$) and baseline ($M = 0.09$, $SD = 0.04$; Bonferroni corrected: $p = 0.006$); the dwell time of State 2 during high-harmfulness idea generation ($M = 2.39$, $SD = 1.69$; $F = 4.55$, $p = 0.014$, $\eta_p^2 = 0.10$) was significantly higher than baseline ($M = 0.1.60$, $SD = 0.79$; Bonferroni corrected: $p = 0.019$).

Discussion

Based on the working neurological model of deception, designing deceptive responses is the core process of scam generation (Mohamed et al., 2006). Given this framework, creativity is crucial. It plays a central role in the successful implementation and long-term effectiveness of a scam (e.g., Walczyk et al., 2008; Walczyk et al., 2005).While Qiao et al. (2023) revealed the brain regions that may be related to lying, the current study conducted a more in-depth investigation to reveal the neural correlates underlying the generation of creative scams (focused on the planning stage) by comparing the differences between high- and low-creativity lying ideas. Additionally, recognizing that not all scams or deceptive behaviors are intended to cause harm (Hunter et al., 2022), the LYT used in the current study were designed to explicitly highlight malevolent intent.

Consistent with the assumption of the working neurological model of

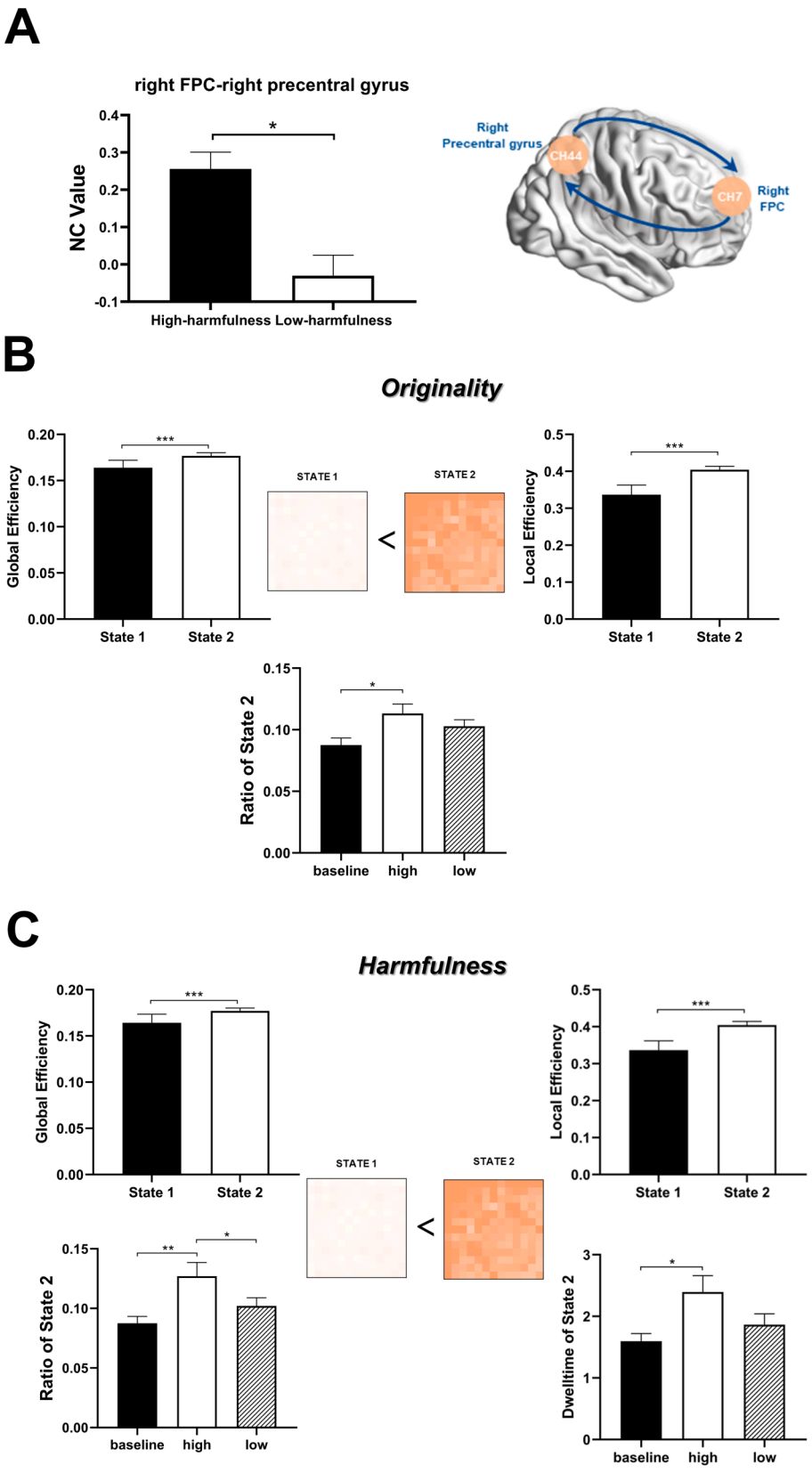

Fig. 4. Results on difference between high- and low-harmfulness scams in neural coupling; NC = neural coupling; FPC = frontopolar cortex; (B) Cluster analysis in baseline, high- and low-originality scams; (C) Cluster analysis in baseline, high- and low-harmfulness scams; $^{*}p < 0.05$, $^{**}p < 0.01$, $^{***}p < 0.001$.

deception, several regions in the bilateral prefrontal cortex and the right temporal lobe were found to be involved in planning creative scams, such as the bilateral FPC, the right DLPFC, the right AG, and the right precuneus (Mohamed et al., 2006). The coupling between the rFPC and the right precentral gyrus was stronger during the generation of high-harmfulness scams than during the generation of low-harmfulness scams. The creativity-related regions (e.g., the left DLPFC and left FPC) were positively involved in creative scams, whereas morality-related regions (e.g., the right DLPFC and right MOG) were negatively involved in creative scams. Moreover, an efficient and dense coupling state was closer to high-creativity scams than low-creativity scams. In summary, the current study validates the findings of Qiao et al. (2023) regarding the role of the rFPC in the generation of creative scams. Additionally, it further identified the involvement of brain regions associated with the weakening of self-control motivations (e.g., right precentral gyrus), enhancement of creative idea generation (e.g., left FPC), and reduction of empathy (e.g., right fusiform) for victims in the process of generating highly creative scams.

The results indicated that several regions in the PFC and the right temporal cortex, which were theoretically hypothesized to be associated with planning deceptive behavior (Mohamed et al., 2006), were involved in both high- and low-creativity scam generation. These findings primarily reveal the role of creativity in scam generation (e.g., Gino and Ariely, 2012; Kapoor and Khan, 2017). Moreover, Perchtold-Stefan et al. (2023) found that stronger frontal cortex activity in the early stages of generating malevolent ideas might be related to inhibiting normative ideas to meet malevolent demands. In contrast, temporal lobe activity was more involved in the mid-stages of generating malevolent ideas, possibly indicating that individuals were attempting to produce unprecedented ideas. During the LYT, the left FPC, right AG, and right precuneus, were significantly activated relative to the baseline. It may be related to applied creativity for malevolent purpose in the LYT (Chen et al., 2015; Green et al., 2015; Perchtold-Stefan et al., 2023; Wertz et al., 2020; Wu et al., 2015; Zhu et al., 2017). Similarly, the decreased activity in right middle temporal gyrus and right superior temporal gyrus reflects higher openness and divergent thinking (Vartanian et al., 2018; Zabelina et al., 2019), which may further implicate the general creation during LYT. Furthermore, a significant activation relative to the baseline was observed in the rFPC. Previous findings revealed that right frontopolar pole was engaged in ToM (Lewis et al., 2011; Reniers et al., 2014), which is an important process to manipulate and predict victims' thoughts during deception (e.g., Sai et al., 2021; Walczyk and Cockrell, 2022; Walczyk et al., 2014). Moreover, the bilateral FPC is related to complex cognitive strategies (Abe, 2011; Ganis et al., 2003; Lin et al., 2021), and the rFPC has been further identified as playing a pivotal role in the construction of well-rehearsed lies (Abe, 2011; Ganis et al., 2003). Qiao et al. (2023) found that rFPC was involved in generating creative scams. The current study used the same dataset as Qiao et al. (2023), and the findings may indicate that activity in the rFPC is associated with an individual's attempt to construct novel and plausible scams. This re-analysis emphasizes the role of the rFPC in malevolent creativity, consistent with the results from Qiao et al. (2023). Additionally, morality is implicated in deception (van 't Veer et al., 2014; Pang et al., 2022; Speer et al., 2020), indicated by significant activation of the right MOG and deactivation of the rDLPFC and rSMG relative to baseline. The activity of right MOG may represent the automatic stimulation of moral judgment functions (Cheng et al., 2021b), whereas reduced activity of rDLPFC and rSMG implicates the focus on selfish demands (Knoch et al., 2006; Silani et al., 2013).

The working neurological model of deception indicates several prefrontal regions related to response control engage in deception planning (Abe, 2011; Mohamed et al., 2006). Results found that the neural coupling between the rFPC and the right precentral gyrus was significantly stronger in the generation of highly harmful scams than in less harmful scams. The rFPC acts as a central role in constructing well-rehearsed lies (Abe, 2011; Ganis et al., 2003). The volume and activity intensity of the right precentral gyrus are negatively associated with impulse control (Yan et al., 2022; Ye et al., 2020). The enhanced coupling between the rFPC and the right precentral gyrus might indicate that a reducing control over immoral thoughts during the generation of creative scams could facilitate their harmfulness. However, there were no significant differences (after FDR correction) in brain activation between the generation of highly and less creative scams. This might suggest that individuals rely more on the inter-regions coupling when generating highly creative scams, potentially involving the interaction of multiple psychological functions. The overall activity level of a single brain region may not reflect the complex interactions involved in the generation of highly creative scams.

In generating malevolent ideas, individuals need to integrate cognitive and emotional information while managing the emotional burden of their creative thoughts (Perchtold-Stefan et al., 2023). Additionally, they also seek to gain extra personal benefits (e.g., Cropley et al., 2010). Thus, emotional processing and controlling selfish motives can be influential in scam generation. The comparison of the task performance-neural activity relationship between high- and low-creativity lying ideas revealed that the activity of the right pre-motor cortex was negatively correlated with originality when generating high-originality scams. The pre-motor cortex is associated with emotional empathy (i.e., the perception of others' emotional states) rather than cognitive empathy (i.e., understanding others' thoughts; Braadbaart et al., 2014; Nummenmaa et al., 2008). Thus, reducing the processing of victims' emotions may facilitate the generation of highly harmful deceptions. Next, the coupling between the rDLPFC and the right fusiform gyrus negatively correlated with originality when generating low-originality scams. The enhanced activity of the rDLPFC can further stimulate the inhibition of selfish motivation (Knoch et al., 2006), while the right fusiform gyrus is associated with empathy (e.g., Rankin et al., 2006; Schmidt et al., 2021). These prosocial functions may intervene more in the generation of low-originality scams than in high-originality scams. Additionally, the coupling between the bilateral DLPFC is significantly positively correlated with the performance of low-novelty scams. The left DLPFC is involved in self-interest maximization (e.g., Liu et al., 2018). This may imply that enhanced self-interested motivation may, to some extent, weaken the inhibitory effect of prosocial functions on scam generation.

Further, the differences in the trait-neural activity relationship between high- and low-creativity lying ideas were examined. LY potential (i.e., trait LY) was significantly positively correlated with the coupling between the left FPC and right precentral gyrus when generating high-originality scams. The left FPC is associated with idea generation (e.g., Zhu et al., 2017), while activity in the right precentral gyrus indicates a reduction in impulse control (Yan et al., 2022; Ye et al., 2020). This might imply that individuals with high LY potential may benefit from the release of impulsivity in constructing high-originality scams, as it facilitates the level of originality. The moral personality was positively correlated with left IFG-right postcentral gyrus coupling in low-harmfulness lying, while it was negatively correlated with left FPC-right precuneus coupling in high-harmfulness lying. Both the left IFG and left PFC are linked to general creation (e.g., Fink et al., 2009; Zhang et al., 2014; Zhu et al., 2017). Antisocial behavior is connected with the reduction of the gray matter volume in right postcentral gyrus (Aoki et al., 2014). Malevolent creation is accompanied by decreased activity in right postcentral gyrus, which may represent the inhibition of emotional perception toward victims (Gao et al., 2022). Previous studies have shown that the precuneus was involved with processing self-image (Kawamichi et al., 2019; Kumar et al., 2019). These results might indicate that individuals with salient moral character have a stronger perception of the victims' emotions when generating creative deceptions, and they are less inclined to link creative deceptive behaviors with their self-concept.

Results of elastic-net regression revealed that the activation of the right MOG negatively predicted the originality of all generated scams.

This may suggest that the inhibition of moral judgement is related to creative deception (Cheng et al., 2021b; Qiao et al., 2022). The left DLPFC, which is related to idea generation (e.g., Zhu et al., 2017), has been found to be positively connected to generating creative scams. Furthermore, the coupling between the left DLPFC and the right precentral gyrus positively predicted the originality during the generation of high-originality scams. For high-harmfulness scams, the coupling between right MOG and right precentral gyrus negatively predicted their harmfulness. The activity of right precentral gyrus is linked to reduction in impulse control, which may be crucial to generating scams (Yan et al., 2022; Ye et al., 2020). The participation of general creativity strengthens the construction of high-creativity scams (i.e., the left DLPFC; e.g., Zhu et al., 2017), whereas the involvement of moral judgement has the opposite effect (i.e., right MOG; Cheng et al., 2021b; Qiao et al., 2022). Additionally, the coupling between the right DLPFC and right fusiform gyrus/ AG negatively predicted originality/harmfulness when generating low-creativity generation. The right AG contribute to malevolent creation (Caspers et al., 2014; Green et al., 2015; Qiao et al., 2023). The enhanced activation of the right DLPFC increases the control of selfish motivation (Knoch et al., 2006), and right fusiform gyrus is positively related to empathy (e.g., Rankin et al., 2006; Schmidt et al., 2021). In summary, reducing selfish motivation and fostering empathy are opposed to the core features of malevolent creativity. These results might imply that the weakening of selfish motivation could impair the quality of creative deceptions.

In general, highly creative scams may require more cognitive resources, thereby mobilizing a more efficient brain state. Clustering analysis has identified two distinct NC states (i.e., State 1 and 2) among baseline, high- and low-creativity scams (including originality and harmfulness). Both global and local efficiency of State 2 was higher than State 1. Several studies have revealed that high global and local efficiency is indicative of enhanced information integration, which further contributed to combining remote ideas to construct creative products (Beaty et al., 2015; Gao et al., 2017; Langer et al., 2012; Wang et al., 2022). Moreover, the ratio and dwell time of State 2 were higher in high-creativity scam generation than in other conditions. A tight and efficient neural coupling state may be crucial for generating high-quality scams.

Several limitations should be acknowledged and discussed: (1) fNIRS only detects the superficial part of the bilateral PFC and the right temporal regions. However, scam creation might also engage subcortical regions. Thus, to uncover the neural underpinnings of scam creation more comprehensively, employing imaging techniques with greater spatial resolution (fMRI and MEG) is recommended; (2) participants were required to generate various scams within a predetermined laboratory setting. Researchers should further design the lying tasks with greater ecological validity; (3) the current study exhibited a gender imbalance within its sample. Future research should investigate the implications of possible gender differences in scam generation; (4) recent studies have indicated that neuroscience studies require larger sample sizes to avoid issues of low statistical power and reduced reproducibility (e.g., Bossier et al., 2020). Future researchers are advised to use sample sizes greater than 40 for task-based brain imaging studies. (5) it is essential to explicitly reaffirm that the data used in this study are identical to those utilized by Qiao et al. (2023). Future meta-analyses and related research should take this into account. For practical applications, the findings of the current study suggest using designed educational programs aimed at reducing creative scams. Enhancing empathy, moral reasoning, and ethical decision-making through targeted training can potentially diminish the use of malevolent creativity in deceptive behaviors. Based on the findings of the current study and the approach suggested by Gao et al. (2023), non-invasive neural modulation techniques to inhibit activity in the rFPC may potentially suppress the generation of novel scams. Additionally, researchers can further explore the cognitive mechanisms by which the rFPC influences the creation of novel scams, thereby clarifying its role and pathways more precisely. This dual approach of modulation and mechanism exploration may provide insights and practical strategies for managing malevolent creativity.

Ethical statement

We have read and have abided by the statement of ethical standards for manuscripts submitted to Neuroscience.

CRediT authorship contribution statement

Xinuo Qiao: Writing – original draft, Visualization, Methodology, Investigation, Formal analysis, Conceptualization. **Wenyu Zhang:** Writing – original draft, Visualization, Formal analysis. **Ning Hao:** Writing – review & editing, Supervision, Resources, Project administration, Methodology, Funding acquisition, Conceptualization.

Declaration of competing interest

The authors declare that they have no known competing financial interests or personal relationships that could have appeared to influence the work reported in this paper.

Acknowledgements

This work was supported by the STI 2030-Major Projects 2021ZD0200500, China, and the Fundamental Research Funds for the Central Universities, China.

References

Abe, N., 2011. How the brain shapes deception: an integrated review of the literature. Neuroscientist 17, 560–574. https://doi.org/10.1177/1073858410393359.
Achard, S., Bullmore, E., 2007. Efficiency and cost of economical brain functional networks. PLoS Comput. Biol. 3, e17.
Aggarwal, C.C., Hinneburg, A., Keim, D.A., 2001. On the surprising behavior of distance metrics in high dimensional space. In: Database Theory—ICDT 2001: 8th International Conference London, UK, January 4–6, 2001 Proceedings 8. Springer, Berlin Heidelberg, pp. 420–434.
Agnoli, S., Corazza, G.E., Runco, M.A., 2016. Estimating creativity with a multiple-measurement approach within scientific and artistic domains. Creat. Res. J. 28, 171–176.
Allen, E.A., Damaraju, E., Plis, S.M., Erhardt, E.B., Eichele, T., Calhoun, V.D., 2014. Tracking whole-brain connectivity dynamics in the resting state. Cereb. Cortex 24, 663–676. https://doi.org/10.1093/cercor/bhs352.
Aoki, Y., Inokuchi, R., Nakao, T., Yamasue, H., 2014. Neural bases of antisocial behavior: a voxel-based meta-analysis. Soc. Cogn. Affect. Neurosci. 9 (8), 1223–1231. https://doi.org/10.1093/scan/nst104.
Bazerman, M.H., Gino, F., 2012. Behavioral ethics: toward a deeper understanding of moral judgment and dishonesty. Ann. Rev. Law Soc. Sci. 8, 85–104. https://doi.org/10.1146/annurev-lawsocsci-102811-173815.
Beaty, R.E., Benedek, M., Kaufman, S.B., Silvia, P.J., 2015. Default and executive network coupling supports creative idea production. Sci. Rep. 5, 10964. https://doi.org/10.1038/srep10964.
Beaty, R.E., Benedek, M., Silvia, P.J., Schacter, D.L., 2016. Creative cognition and brain network dynamics. Trends Cogn. Sci. 20 (2), 87–95. https://doi.org/10.1016/j.tics.2015.10.004.
Beaty, R.E., Christensen, A.P., Benedek, M., Silvia, P.J., Schacter, D.L., 2017. Creative constraints: brain activity and network dynamics underlying semantic interference during idea production. Neuroimage 148, 189–196. https://doi.org/10.1016/j.neuroimage.2017.01.012.
Beaty, R.E., Kenett, Y.N., Christensen, A.P., Rosenberg, M.D., Benedek, M., Chen, Q., Fink, A., Qiu, J., Kwapil, T.R., Kane, M.J., Silvia, P.J., 2018. Robust prediction of individual creative ability from brain functional connectivity. Proc. Natl. Acad. Sci. 115, 1087–1092. https://doi.org/10.1073/pnas.1713532115.
Bossier, H., Roels, S.P., Seurinck, R., Banaschewski, T., Barker, G.J., Bokde, A.L., et al., 2020. The empirical replicability of task-based fMRI as a function of sample size. Neuroimage 212, 116601. https://doi.org/10.1016/j.neuroimage.2020.116601.
Braadbaart, L., de Grauw, H., Perrett, D.I., Waiter, G.D., Williams, J.H.G., 2014. The shared neural basis of empathy and facial imitation accuracy. Neuroimage 84, 367–375. https://doi.org/10.1016/j.neuroimage.2013.08.061.
Carrington, S.J., Bailey, A.J., 2009. Are there theory of mind regions in the brain? A review of the neuroimaging literature. Hum. Brain Mapp. 30 (8), 2313–2335. https://doi.org/10.1002/hbm.20671.
Caspers, J., Zilles, K., Amunts, K., Laird, A.R., Fox, P.T., Eickhoff, S.B., 2014. Functional characterization and differential coactivation patterns of two cytoarchitectonic visual areas on the human posterior fusiform gyrus. Hum. Brain Mapp. 35 (6), 2754–2767. https://doi.org/10.1002/hbm.22364.

Chen, C., Zhou, J., Liu, C., Witt, K., Zhang, Y., Jing, B., et al., 2015. Regional homogeneity of resting-state brain abnormalities in violent juvenile offenders: a biomarker of brain immaturity? J. Neuropsychiatry Clin. Neurosci. 27, 27–32. https://doi.org/10.1176/appi.neuropsych.13030044.

Cheng, R., Lu, K., Hao, N., 2021b. The effects of anger on different forms of malevolent creative performance. J. Psychol. Sci. 44, 1336–1345. https://doi.org/10.16719/j.cnki.1671-6981.20210608.

Chow, S., Shao, J., Wang, H., Lokhnygina, Y., 2017. In: Sample Size Calculations in Clinical Research. CRC Press. https://doi.org/10.1201/9781315183084.

Cropley, D.H., Kaufman, J.C., Cropley, A.J., 2008. Malevolent creativity: a functional model of creativity in terrorism and crime. Creat. Res. J. 20 (2), 105–115. https://doi.org/10.1080/10400410802059424.

Cropley, D.H., Cropley, A.J., Kaufman, J.C., Runco, M.A., 2010. The Dark Side of Creativity. Cambridge University Press.

Cui, X., Bray, S., Reiss, A.L., 2010. Functional near infrared spectroscopy (NIRS) signal improvement based on negative correlation between oxygenated and deoxygenated hemoglobin dynamics. Neuroimage 49, 3039–3046. https://doi.org/10.1016/j.neuroimage.2009.11.050.

Cui, X., Bryant, D.M., Reiss, A.L., 2012. NIRS-based hyperscanning reveals increased interpersonal coherence in superior frontal cortex during cooperation. Neuroimage 59, 2430–2437. https://doi.org/10.1016/j.neuroimage.2011.09.003.

Cui, F., Wu, S., Wu, H., Wang, C., Jiao, C., Luo, Y., 2018. Altruistic and self- serving goals modulate behavioral and neural responses in deception. Soc. Cogn. Affect. Neurosci. 13 (1), 63–71. https://doi.org/10.1093/scan/nsx138.

DePaulo, B.M., Lindsay, J.J., Malone, B.E., Muhlenbruck, L., Charlton, K., Cooper, H., 2003. Cues to deception. Psychol. Bull. 129 (1), 74–118. https://doi.org/10.1037/0033-2909.129.1.74.

Du, W., Chen, M., 2023. Too much or less? The effect of financial literacy on resident fraud victimization. Comput. Hum. Behav. 148, 107914 https://doi.org/10.1016/j.chb.2023.107914.

European Commission, 2020. Survey on “scams and fraud experienced by consumers”: Final report. https://ec.europa.eu/info/sites/info/files/aid_development_cooperation_fundamental_rights/ensuring_aid_effectiveness/documents/survey_on_scams_and_fraud_experienced_by_consumers_-_final_report.pdf.

Fang, F., Potter, T., Nguyen, T., Zhang, Y., 2020. Dynamic reorganization of the cortical functional brain network in affective processing and cognitive reappraisal. Int. J. Neural Syst. 30, 2050051. https://doi.org/10.1142/S0129065720500513.

Fink, A., Grabner, R.H., Benedek, M., Reishofer, G., Hauswirth, V., Fally, M., Neuper, C., Ebner, F., Neubauer, A.C., 2009. The creative brain: investigation of brain activity during creative problem solving by means of EEG and FMRI. Hum. Brain Mapp. 30 (3), 734–748. https://doi.org/10.1002/hbm.20538.

Fink, A., Grabner, R.H., Gebauer, D., Reishofer, G., Koschutnig, K., Ebner, F., 2010. Enhancing creativity by means of cognitive stimulation: evidence from an fMRI study. Neuroimage 52 (4), 1687–1695. https://doi.org/10.1016/j.neuroimage.2010.05.072.

Ganis, G., Kosslyn, S.M., Stose, S., Thompson, W.L., Yurgelun-Todd, D.A., 2003. Neural correlates of different types of deception: an fMRI investigation. Cereb. Cortex 13, 830–836. https://doi.org/10.1093/cercor/13.8.830.

Gao, Z., Lu, K., Hao, N., 2023. Transcranial direct current stimulation (tDCS) targeting the postcentral gyrus reduces malevolent creative ideation. Social Cognitive and Affective Neuroscience 18, nsad019. https://doi.org/10.1093/scan/nsad019.

Gao, Z., Zhang, D., Liang, A., Liang, B., Wang, Z., Cai, Y., et al., 2017. Exploring the associations between intrinsic brain connectivity and creative ability using functional connectivity strength and connectome analysis. Brain Connect. 7, 590–601. https://doi.org/10.1089/brain.2017.0510.

Gao, Z., Cheng, L., Li, J., Chen, Q., Hao, N., 2022. The dark side of creativity: neural correlates of malevolent creative idea generation. Neuropsychologia 167, 108164. https://doi.org/10.1016/j.neuropsychologia.2022.108164.

Gaspar, J.P., Methasani, R., Schweitzer, M.E., 2022. Deception in negotiations: insights and opportunities. Curr. Opin. Psychol. 47, 101436 https://doi.org/10.1016/j.copsyc.2022.101436.

Gee, J., Button, M., 2019. The financial cost of fraud 2019. http://www.crowe.ie/wp-content/uploads/2019/08/The-Financial-Cost-of-Fraud-2019.pdf.

Gill, P., Horgan, J., Hunter, S.T., Cushenbery, D.L., 2013. Malevolent creativity in terrorist organizations. J. Creat. Behav. 47 (2), 125–151. https://doi.org/10.1002/jocb.28.

Gino, F., Ariely, D., 2012. The dark side of creativity: original thinkers can be more dishonest. J. Pers. Soc. Psychol. 102, 445–459. https://doi.org/10.1037/a0026406.

Green, A.E., Cohen, M.S., Raab, H.A., Yedibalian, C.G., Gray, J.R., 2015. Frontopolar activity and connectivity support dynamic conscious augmentation of creative state. Hum. Brain Mapp. 36, 923–934. https://doi.org/10.1002/hbm.22676.

Hanoch, Y., Wood, S., 2021. The scams among us: who falls prey and why. Curr. Dir. Psychol. Sci. 30, 260–266. https://doi.org/10.1177/0963721421995489.

Hao, N., Tang, M., Yang, J., Wang, Q., Runco, M.A., 2016. A new tool to measure malevolent creativity: the malevolent creativity behavior scale. Front. Psychol. 7, 00682. https://doi.org/10.3389/fpsyg.2016.00682.

Harris, D.J., Reiter-Palmon, R., Kaufman, J.C., 2013. The effect of emotional intelligence and task type on malevolent creativity. Psychol. Aesthet. Creat. Arts 7 (3), 237–244. https://doi.org/10.1037/a0032139.

He, Y., Dagher, A., Chen, Z., Charil, A., Zijdenbos, A., Worsley, K., Evans, A., 2009. Impaired small-world efficiency in structural cortical networks in multiple sclerosis associated with white matter lesion load. Brain 132, 3366–3379. https://doi.org/10.1093/brain/awp089.

Hunter, S.T., Walters, K., Nguyen, T., Manning, C., Miller, S., 2022. Malevolent creativity and malevolent innovation: a critical but tenuous linkage. Creat. Res. J. 34, 123–144. https://doi.org/10.1080/10400419.2021.1987735.

Jang, K.E., Tak, S., Jung, J., Jang, J., Jeong, Y., Ye, J.C., 2009. Wavelet minimum description length detrending for near-infrared spectroscopy. J. Biomed. Opt. 14, 0340013. https://doi.org/10.1117/1.3127204.

Jenkins, A.C., Zhu, L., Hsu, M., 2016. Cognitive neuroscience of honesty and deception: a signaling framework. Curr. Opin. Behav. Sci. 11, 130–137. https://doi.org/10.1016/j.cobeha.2016.09.005.

Jiang, L., Yang, Q., He, R., Wang, G., Yi, C., Si, Y., Yao, D., Xu, P., Yu, L., Li, F., 2023. Edge-centric functional network predicts risk propensity in economic decision-making: evidence from a resting-state fMRI study. Cereb. Cortex 33, 8904–8912. https://doi.org/10.1093/cercor/bhad169.

Kapoor, H., Kaufman, J.C., 2022. The evil within: the AMORAL model of dark creativity. Theory Psychol. 32 (3), 467–490. https://doi.org/10.1177/09593543221074326.

Kapoor, H., Khan, A., 2017. Deceptively yours: valence-based creativity and deception. Think. Skills Creat. 23, 199–206. https://doi.org/10.1016/j.tsc.2016.12.006.

Kawamichi, H., Sugawara, S.K., Hamano, Y.H., Makita, K., Kochiyama, T., Kikuchi, Y., Ogino, Y., Saito, S., Sadato, N., 2019. Prosocial behavior toward estranged persons modulates the interaction between midline cortical structures and the reward system. Soc. Neurosci. 14 (5), 618–630. https://doi.org/10.1080/17470919.2018.1553797.

Knoch, D., Pascual-Leone, A., Meyer, K., Treyer, V., Fehr, E., 2006. Diminishing reciprocal fairness by disrupting the right prefrontal cortex. Science 314 (5800), 829–832. https://doi.org/10.1126/science.1129156.

Kumar, P., Pisoni, A., Bondy, E., Kremens, R., Singleton, P., Pizzagalli, D.A., Auerbach, R. P., 2019. Delineating the social valuation network in adolescents. Soc. Cogn. Affect. Neurosci. 14 (11), 1159–1166. https://doi.org/10.1093/scan/nsz086.

Langer, N., Pedroni, A., Gianotti, L.R., Hänggi, J., Knoch, D., Jäncke, L., 2012. Functional brain network efficiency predicts intelligence. Hum. Brain Mapp. 33, 1393–1406. https://doi.org/10.1002/hbm.21297.

Lee, K., Ashton, M.C., 2004. Psychometric properties of the HEXACO personality inventory. Multivar. Behav. Res. 39, 329–358. https://doi.org/10.1207/s15327906mbr3902_8.

Lewis, P.A., Rezaie, R., Brown, R., Roberts, N., Dunbar, R.I.M., 2011. Ventromedial prefrontal volume predicts understanding of others and social network size. Neuroimage 57, 1624–1629. https://doi.org/10.1016/j.neuroimage.2011.05.030.

Li, R., Mayseless, N., Balters, S., Reiss, A.L., 2021. Dynamic inter-brain synchrony in real-life inter-personal cooperation: a functional near-infrared spectroscopy hyperscanning study. Neuroimage 238, 118263. https://doi.org/10.1016/j.neuroimage.2021.118263.

Lin, X.A., Wang, C., Zhou, J., Sai, L., Fu, G., 2021. Neural correlates of spontaneous deception in a non-competitive interpersonal scenario: a functional near-infrared spectroscopy (fNIRS) study. Brain Cogn. 150, 105704. https://doi.org/10.1016/j.bandc.2021.105704.

Lisofsky, N., Kazzer, P., Heekeren, H.R., Prehn, K., 2014. Investigating socio-cognitive processes in deception: a quantitative meta-analysis of neuroimaging studies. Neuropsychologia 61, 113–122. https://doi.org/10.1016/j.neuropsychologia.2014.06.001.

Liu, G., Zeng, G., Wang, F., Rotshtein, P., Peng, K., Sui, J., 2018. Praising others differently: neuroanatomical correlates to individual differences in trait gratitude and elevation. Soc. Cogn. Affect. Neurosci. 13, 1225–1234. https://doi.org/10.1093/scan/nsy093.

Lu, K., Xue, H., Nozawa, T., Hao, N., 2019. Cooperation makes a group be more creative. Cereb. Cortex 29, 3457–3470. https://doi.org/10.1093/cercor/bhy215.

Mai, K.M., Ellis, A.P.J., Welsh, D.T., 2015. The gray side of creativity: exploring the role of activation in the link between creative personality and unethical behavior. J. Exp. Soc. Psychol. 60, 76–85. https://doi.org/10.1016/j.jesp.2015.05.004.

Mohamed, F.B., Faro, S.H., Gordon, N.J., Platek, S.M., Ahmad, H., Williams, J.M., 2006. Brain mapping of deception and truth telling about an ecologically valid situation: functional MR imaging and polygraph investigation–initial experience. Radiology 238, 679–688. https://doi.org/10.1148/radiol.2382050237.

Nummenmaa, L., Hirvonen, J., Parkkola, R., Hietanen, J.K., 2008. Is emotional contagion special? An fMRI study on neural systems for affective and cognitive empathy. Neuroimage 43 (3), 571–580. https://doi.org/10.1016/j.neuroimage.2008.08.014.

Pan, Y., Novembre, G., Song, B., Li, X., Hu, Y., 2018. Interpersonal synchronization of inferior frontal cortices tracks social interactive learning of a song. Neuroimage 183, 280–290. https://doi.org/10.1016/j.neuroimage.2018.08.005.

Pang, L., Li, H., Liu, Q., Luo, Y.J., Mobbs, D., Wu, H., 2022. Resting-state functional connectivity of social brain regions predicts motivated dishonesty. Neuroimage 256, 119253. https://doi.org/10.1016/j.neuroimage.2022.119253.

Perchtold-Stefan, C.M., Fink, A., Rominger, C., Papousek, I., 2020. Creative, antagonistic, and angry? Exploring the roots of malevolent creativity with a Real-World idea generation task. J. Creat. Behav. 55, 710–722. https://doi.org/10.1002/jocb.484.

Perchtold-Stefan, C.M., Fink, A., Rominger, C., Szabó, E., Papousek, I., 2022. Enjoying others’ distress and indifferent to threat? Changes in prefrontal-posterior coupling during social-emotional processing are linked to malevolent creativity. Brain Cogn. 163, 105913 https://doi.org/10.1016/j.bandc.2022.105913.

Perchtold-Stefan, C.M., Rominger, C., Papousek, I., Fink, A., 2023. Functional EEG alpha activation patterns during malevolent creativity. Neuroscience 522, 98–108. https://doi.org/10.1016/j.neuroscience.2023.05.006.

Pinti, P., Devoto, A., Greenhalgh, I., Tachtsidis, I., Burgess, P.W., de C Hamilton, Antonia F., 2021. The role of anterior prefrontal cortex (area 10) in face-to-face deception measured with fNIRS. Soc. Cogn. Affect. Neurosci. 16 (1–2), 129–142. https://doi.org/10.1093/scan/nsaa086.

Qiao, X., Lu, K., Teng, J., Gao, Z., Hao, N., 2022. Middle occipital area differentially associates with malevolent versus benevolent creativity: an fNIRS investigation. Soc. Neurosci. 17, 127–142. https://doi.org/10.1080/17470919.2022.2038261.

Qiao, X., Lu, K., Yun, Q., Hao, N., 2023. Similarities and distinctions between cortical neural substrates that underlie generation of malevolent creative ideas. eNeuro 10, 1–15. https://doi.org/10.1523/ENEURO.0127-23.2023.
Rankin, K.P., Gorno-Tempini, M.L., Allison, S.C., Stanley, C.M., Glenn, S., Weiner, M.W., Miller, B.L., 2006. Structural anatomy of empathy in neurodegenerative disease. Brain 129, 2945–2956. https://doi.org/10.1093/brain/awl254.
Ren, J., Huang, F., Gao, C., Gott, J., Schoch, S.F., Qin, S., Dresler, M., Luo, J., 2023. Functional lateralization of the medial temporal lobe in novel associative processing during creativity evaluation. Cereb. Cortex 33, 1186–1206. https://doi.org/10.1093/cercor/bhac129.
Reniers, R.L.E.P., Völlm, B.A., Elliott, R., Corcoran, R., 2014. Empathy, ToM, and self-other differentiation: an fMRI study of internal states. Soc. Neurosci. 9, 50–62. https://doi.org/10.1080/17470919.2013.861360.
Runco, M.A., Abdulla, A.M., Paek, S.H., Al-Jasim, F.A., Alsuwaidi, H.N., 2016. Which test of divergent thinking is best? Creativity: Theories – Res. – Appl. 3, 4–18. https://doi.org/10.1515/ctra-2016-0001.
Runco, M.A., Okuda, S.M., 1991. The instructional enhancement of the flexibility and originality scores of divergent thinking tests. Appl. Cogn. Psychol. 5, 435–441. https://doi.org/10.1002/acp.2350050505.
Sai, L., Zhou, X., Ding, X., 2014. Detecting concealed information using functional near-infrared spectroscopy. Brain Topogr. 27, 652–662. https://doi.org/10.1007/s10548-014-0352-z.
Sai, L., Shang, S., Tay, C., Liu, X., Sheng, T., Fu, G., Ding, X.P., Lee, K., 2021. Theory of mind, executive function, and lying in children: a meta-analysis. Dev. Sci. 24, e13096.
Schecklmann, M., Ehlis, A.C., Plichta, M.M., Fallgatter, A.J., 2010. Influence of muscle activity on brain oxygenation during verbal fluency assessed with functional near-infrared spectroscopy. Neuroscience 171 (2), 434–442. https://doi.org/10.1016/j.neuroscience.2010.08.072.
Schmidt, S.N.L., Hass, J., Kirsch, P., Mier, D., 2021. The human mirror neuron system—A common neural basis for social cognition? Psychophysiology 58, e13781-n/a. https://doi.org/10.1111/psyp.13781.
Schweitzer, M.E., Hershey, J.C., Bradlow, E.T., 2006. Promises and lies: restoring violated trust. Organ. Behav. Hum. Decis. Process. 101 (1), 1–19. https://doi.org/10.1016/j.obhdp.2006.05.005.
Silani, G., Lamm, C., Ruff, C.C., Singer, T., 2013. Right supramarginal gyrus is crucial to overcome emotional egocentricity bias in social judgments. J. Neurosci. 33, 15466–15476. https://doi.org/10.1523/JNEUROSCI.1488-13.2013.
Singh, A.K., Okamoto, M., Dan, H., Jurcak, V., Dan, I., 2005. Spatial registration of multichannel multi-subject fNIRS data to MNI space without MRI. Neuroimage 27, 842–851. https://doi.org/10.1016/j.neuroimage.2005.05.019.
Speer, S.P.H., Smidts, A., Boksem, M.A.S., 2020. Cognitive control increases honesty in cheaters but cheating in those who are honest. Proc. Natl. Acad. Sci. 117 (32), 19080–19091. https://doi.org/10.1073/pnas.2003480117.
Speer, S.P.H., Smidts, A., Boksem, M.A.S., 2022. Individual differences in (dis)honesty are represented in the brain's functional connectivity at rest. Neuroimage 246, 118761. https://doi.org/10.1016/j.neuroimage.2021.118761.
Takeuchi, N., Mori, T., Suzukamo, Y., Izumi, S.I., 2019. Activity of prefrontal cortex in teachers and students during teaching of an insight problem. Mind Brain Educ. 13, 167–175. https://doi.org/10.1111/mbe.12207.
Tempest, G.D., Radel, R., 2019. Put on your (fNIRS) thinking cap: frontopolar activation during augmented state creativity. Behav. Brain Res. 373, 112082 https://doi.org/10.1016/j.bbr.2019.112082.
Thijssen, S., Wildeboer, A., van IJzendoorn, M.H., Muetzel, R.L., Langeslag, S.J.E., Jaddoe, V.W.V., Verhulst, F.C., Tiemeier, H., Bakermans-Kranenburg, M.J., White, T., 2017. The honest truth about deception: demographic, cognitive, and neural correlates of child repeated deceptive behavior. J. Exp. Child Psychol. 162, 225–241. https://doi.org/10.1016/j.jecp.2017.05.009.
Tsuzuki, D., Jurcak, V., Singh, A.K., Okamoto, M., Watanabe, E., Dan, I., 2007. Virtual spatial registration of stand-alone fNIRS data to MNI space. Neuroimage 34, 1506–1518. https://doi.org/10.1016/j.neuroimage.2006.10.043.
van't Veer, Anna E., Stel, M., van Beest, I., 2014. Limited capacity to lie: cognitive load interferes with being dishonest. Judgm. Decis. Mak. 9 (3), 199–206. https://doi.org/10.1017/S1930297500005751.
Vartanian, O., Wertz, C.J., Flores, R.A., Beatty, E.L., Smith, I., Blackler, K., Lam, Q., Jung, R.E., 2018. Structural correlates of openness and intellect: implications for the contribution of personality to creativity. Hum. Brain Mapp. 39, 2987–2996. https://doi.org/10.1002/hbm.24054.
Vrij, A., Granhag, P.A., Porter, S., 2010. Pitfalls and opportunities in nonverbal and verbal lie detection. Psychol. Sci. Public Interest 11 (3), 89–121. https://doi.org/10.1177/1529100610390861.
Walczyk, J.J., Cockrell, N.F., 2022. To err is human but not deceptive. Mem. Cogn. 50 (1), 232–244. https://doi.org/10.3758/s13421-021-01197-8.
Walczyk, J.J., Schwartz, J.P., Clifton, R., Adams, B., Wei, M.I.N., Zha, P., 2005. Lying person-to-person about life events: a cognitive framework for lie detection. Pers. Psychol. 58 (1), 141–170. https://doi.org/10.1111/j.1744-6570.2005.00484.x.
Walczyk, J.J., Runco, M.A., Tripp, S.M., Smith, C.E., 2008. The creativity of lying: divergent thinking and ideational correlates of the resolution of social dilemmas. Creat. Res. J. 20 (3), 328–342. https://doi.org/10.1080/10400410802355152.
Walczyk, J.J., Harris, L.L., Duck, T.K., Mulay, D., 2014. A social-cognitive framework for understanding serious lies: activation-decision-construction-action theory. New Ideas Psychol. 34, 22–36. https://doi.org/10.1016/j.newideapsych.2014.03.001.
Wang, L., 2019. Creativity as a pragmatic moral tool. J. Bus. Res. 96, 1–13. https://doi.org/10.1016/j.jbusres.2018.10.009.
Wang, X., Lu, K., He, Y., Gao, Z., Hao, N., 2022. Close spatial distance and direct gaze bring better communication outcomes and more intertwined neural networks. Neuroimage 261, 119515. https://doi.org/10.1016/j.neuroimage.2022.119515.
Wang, J., Wang, X., Xia, M., Liao, X., Evans, A., He, Y., 2015. GRETNA: a graph theoretical network analysis toolbox for imaging connectomics. Front. Hum. Neurosci. 9, 386. https://doi.org/10.3389/fnhum.2015.00386.
Wertz, C.J., Chohan, M.O., Flores, R.A., Jung, R.E., 2020. Neuroanatomy of creative achievement. Neuroimage 209, 116487. https://doi.org/10.1016/j.neuroimage.2019.116487.
Wu, X., Yang, W., Tong, D., Sun, J., Chen, Q., Wei, D., Zhang, Q., Zhang, M., Qiu, J., 2015. A meta-analysis of neuroimaging studies on divergent thinking using activation likelihood estimation. Hum. Brain Mapp. 36, 2703–2718. https://doi.org/10.1002/hbm.22801.
Xie, H., Beaty, R.E., Jahanikia, S., Geniesse, C., Sonalkar, N.S., Saggar, M., 2021. Spontaneous and deliberate modes of creativity: multitask eigen-connectivity analysis captures latent cognitive modes during creative thinking. Neuroimage 243, 118531. https://doi.org/10.1016/j.neuroimage.2021.118531.
Xie, C., Luchini, S., Beaty, R.E., Du, Y., Liu, C., Li, Y., 2022. Automated creativity prediction using natural language processing and resting-state functional connectivity: an fNIRS study. Creat. Res. J. 34, 401–418. https://doi.org/10.1080/10400419.2022.2108265.
Xue, H., Lu, K., Hao, N., 2018. Cooperation makes two less-creative individuals turn into a highly-creative pair. Neuroimage 172, 527–537. https://doi.org/10.1016/j.neuroimage.2018.02.007.
Yan, H., Shan, X., Li, H., Liu, F., Guo, W., 2022. Abnormal spontaneous neural activity as a potential predictor of early treatment response in patients with obsessive–compulsive disorder. J. Affect. Disord. 309, 27–36. https://doi.org/10.1016/j.jad.2022.04.125.
Ye, J.C., Tak, S., Jang, K.E., Jung, J., Jang, J., 2009. NIRS-SPM: statistical parametric mapping for near-infrared spectroscopy. Neuroimage 44, 428–447. https://10.1016/j.neuroimage.2008.08.036.
Ye, Q., Zhang, Z., Fan, Q., Li, Y., 2020. Altered intramodular functional connectivity in drug naive obsessive-compulsive disorder patients. In: *2020 42nd Annual International Conference of the IEEE Engineering in Medicine & Biology Society (EMBC)*. IEEE, pp. 1734–1737.
Yin, L., Reuter, M., Weber, B., 2016. Let the man choose what to do: neural correlates of spontaneous lying and truth-telling. Brain Cogn. 102, 13–25. https://doi.org/10.1016/j.bandc.2015.11.007.
Zabelina, D.L., Hechtman, L.A., Saporta, A., Grunewald, K., Beeman, M., 2019. Brain activity sensitive to visual congruency effects relates to divergent thinking. Brain Cogn. 135, 103587 https://doi.org/10.1016/j.bandc.2019.103587.
Zhang, H., Liu, J., Zhang, Q., 2014. Neural representations for the generation of inventive conceptions inspired by adaptive feature optimization of biological species. Cortex 50, 162–173. https://doi.org/10.1016/j.cortex.2013.01.015.
Zheltyakova, M., Korotkov, A., Cherednichenko, D., Kireev, M., 2022. Functional interactions between neural substrates of socio-cognitive mechanisms involved in simple deception and manipulative truth. Brain Connect. 12 (7), 639–649. https://doi.org/10.1016/j.cortex.2023.09.018.
Zhu, W., Chen, Q., Xia, L., Beaty, R.E., Yang, W., Tian, F., Sun, J., Cao, G., Zhang, Q., Chen, X., Qiu, J., 2017. Common and distinct brain networks underlying verbal and visual creativity. Hum. Brain Mapp. 38 (4), 2094–2111. https://doi.org/10.1002/hbm.23507.
Zou, H., Hastie, T., 2005. Regularization and variable selection via the elastic net. J. R. Stat. Soc. Ser. B (Stat. Methodol.) 67, 301–320. https://doi.org/10.1111/j.1467-9868.2005.00503.x.